

# Comparative Analysis of Heat Transfer Coefficients in Plain Tube and Twisted Tube Radiators with Variable Mass Flow Rates Using $\text{Al}_2\text{O}_3$ -Water and CuO-Water Nanofluids

Md. Naushad Alam<sup>1\*</sup>, Akash Langde<sup>2</sup>

<sup>1\*</sup>Research Scholar and Assistant Professor, Mechanical Engineering Department, Anjuman College of Engineering and Technology, Nagpur, Maharashtra, India. 440001.

<sup>2</sup>Professor, Mechanical Engineering Department, Anjuman College of Engineering and Technology, Nagpur, Maharashtra, India. 440001.

\* Corresponding Author

## Abstract

This study compares heat transfer coefficients in Plain Tube and Twisted tube radiators utilizing  $\text{Al}_2\text{O}_3$ -water and CuO-water nanofluids at different mass flow rates. The enhancement of heat transfer in automotive cooling systems improves engine efficiency and performance. In present work,  $\text{Al}_2\text{O}_3$ -water and CuO-water nanofluids were prepared and tested in automobile radiator experimental set-up at varying mass flow rates. Experimental results show nanofluids increase heat transfer coefficients over water-based coolants. CuO-water outperformed  $\text{Al}_2\text{O}_3$ -water at higher mass flow rates. The findings suggest that optimizing nanofluid and flow conditions can improve automobile cooling systems. This study provides valuable inputs for the design and operation of advanced radiator systems, improving thermal management tactics in automotive applications.

**Keywords:** Heat transfer coefficient, Twisted Tube radiator,  $\text{Al}_2\text{O}_3$  nanofluid, CuO nanofluid, Mass flow rate, cooling systems

## Introduction:

Automobile engine cooling relies on the radiator. It ensures the engine operates within normal temperatures [1]. Its heat transfer performance affects engine life and vehicle stability. Cars employ fin-and-tube radiators for heat transfer and ease of production [2]. Researchers are focused on heat transmission efficiency and vehicle radiator capacity reduction to conserve energy and reduce consumption. This can be solved actively or passively [3, 4]. Active methods improve heat transfer by using external force or equipment, which increases energy use and expense [5]. Altering the cooling medium's thermophysical characteristics or radiator tube flow field structure implements the passive technique [6–8].

Ethylene glycol ( $\text{C}_2\text{O}_6\text{H}_2$ ) and water ( $\text{H}_2\text{O}$ ) are common radiator coolants [9]. Due to higher compression ratios and engine cylinders, radiator efficiency has decreased. Thus, research on heat transfer coolants that are more widely available, environmentally friendly, and have a high specific heat is growing [10–12]. However, nanofluid coolants improve radiator efficiency [13–15].

Ponangi, et. al., [16] tested a liquid-air vehicle radiator using new hybrid nanoparticles, graphene oxide, and low-volume carboxyl graphene. The results show that the liquid air automotive radiator's effectiveness (232% improvement) and pressure drop (66% reduction) have improved. Hybrid nanoparticles and functionalized graphene boost radiator efficiency [17]. Another study tested an automotive radiator's heat transmission using Multiwalled Carbon Nanotube Nanoparticles (MWCNT) in a 50:50 volume ratio of water and ethylene glycol. The results showed that nanoparticle concentration improves radiator heat transmission. After the experiment, nanoparticle aggregation and sedimentation increased significantly [18]. Charyulu et al. [19] examined how materials affect diesel engine radiator tube and fin manufacture. They found that brass, copper, and carbon steel exhibited comparable HT and PD characteristics. The optimal engine radiator size for equal operating conditions was examined by Rahmatinejad et al. [20]. A genetic algorithm is employed to verify the experimental results. The heat exchanger's size, cost, and weight are

considerably reduced when the number of fins is 436 and the size is 2.867 mm. The hybrid nanofluid's HT efficacy in a circular conduit with wire coil inserts was investigated by Hamid et al. [21]. For  $\text{TiO}_2\text{-SiO}_2$  hybrid nanofluids with a volumetric concentration of 0.5–3.0%, a pitch ratio of 0.83–4.17, and a Re number of 2300–12000, the results are presented. It is reported that the optimal performance is achieved with a pitch ratio of 1.5 and a concentration of 2.5%. For evaluating a temperature and velocity fluctuations of radiator tubes, Akpobi et al. [22] implemented a finite element method (FEM) analysis. They stated that dense meshing is necessary into area of inlets and outflows for achieving precise solutions. Bilen et al. [23] examined a HT characteristics and grooved tube friction in the turbulent flow regime. The comparison of three distinct groove geometries revealed that trapezoidal grooves outperformed circular tubes upto  $\text{Re}=30000$ , while rectangular grooves outperformed them upto  $\text{Re}=28000$ . For all groove geometries, the optimal entropy generation is reported at  $\text{Re}=17000$ . The PD and HT of plane twisted and square cut twisted tube inserts were studied in a turbulent flow regime by Murugesan et al. [24]. The Reynolds number of the tapes ranges from 2000 to 12000 having three twist ratios ( $\gamma = 2.0, 4.4, \text{ and } 6.0$ ). While square cut tape inserts performed far better in HT, they also had a much higher PD than plain cut tape inserts [25]. In the same vein, they presented the formulae for the friction coefficient and the Nusselt number as they pertain to plane and square twisted tapes. Eiamsa-Ard et al. [26] investigated a turbulent heat transfer characteristics of rib fluted tube flow under a uniform heat flux. Triangular rib, crevice, and rectangular rib were compared in order to modify their configurations. The combination of the rectangular rib and the triangular groove outperformed other combinations when it came to hydrothermal performance. Additionally, in order to derive equations for the enhancement index, friction coefficient and Nusselt number, the effect of pitch ratio was studied [27]. According to Loahalerdecha et al. [28], experimental studies are carried out to analyse the friction properties and heat transfer of R-134a in heat exchanger with corrugated pipes. The experimental conditions

included Re numbers from 3500 to 18000 and a constant hot water Re number of 5500. Changing the arrangement of the convex and concave corrugated tubes yields the best results for the version of the pipe with the concave outer corrugation and the convex inner corrugation [29]. In order to modify the mass flows and pitch heights of R-134-a, Ji et al. [30] compared heat exchangers with corrugated tubes and those with flat tubes. Compared to the plain variant, the corrugated pipe was shown to have better hydro-thermal effectiveness. Mohammed et al. [31] conducted a literature review that compared the hydro-thermal performance of various pipe geometries. Internally finned tubes fared better than other tube designs, while corrugated and dimpled pipes PD increase is minor related to thermal enhancement [32]. Lastly, twisted tape inserts performed poorly, especially during the turbulent regime [33]. Ajeel et al. [34] numerically investigate the zigzag and symmetry shape of trapezoidal corrugated tubes. For a concentration range of 1–4%, an aspect ratio of groove of 0.5–4, and  $500 < \text{Re} < 20000$ , four nanofluids ( $\text{Al}_2\text{O}_3$ ,  $\text{CuO}$ ,  $\text{SiO}_2$ , and  $\text{ZnO}$ ) are compared. Trapezoidal grooves demonstrated superior thermal performance, while  $\text{SiO}_2$  exhibited the greatest Nusselt's number. Glycerin is the primary fluid that exhibits the highest level of performance [35]. Kcheril and Elias [36] conducted an experimental investigation to compare the efficacy of nanosized ferro fluids and aluminum-based nanofluids in automobile engines. Ferrofluids demonstrated superior heat transfer capabilities when contrasted with aluminium nanofluids [37]. To enhance the efficiency and minimise the weight and size of radiator Salamon et al. [38] conducted an experimental investigation of the  $\text{TiO}_2$  nano fluid. The standard EG/water blend worked better at low inlet coolant temperatures they found. The  $\text{TiO}_2$  nano fluid increased HT rate by 8.5% over the EG/water mixture at higher temperatures. Goudarziet al. [39] tested  $\text{Al}_2\text{O}_3\text{-EG}$  nanofluid upon vehicle heat exchangers. Investigations are conducted with three increasing concentrations of nanofluids and two wire cross sections that are dissimilar. The utilisation of nanofluids and wire inserts in tandem resulted in a 5% improvement in performance compared to the use of only wire

inserts. The energy elimination requirements of high-performance vehicle engines are significantly higher. Said et al. [40] tested radiators using  $\text{Al}_2\text{O}_3$  and  $\text{TiO}_2$ . They compared thermophysical properties and long-term stability of the two nanofluids. The  $\text{Al}_2\text{O}_3$  /EG:DW increased thermal effectiveness by 24.21%. Shahsavani et al. [41] used real data to develop a succinct correlation function of particle concentration and temperature for F-MWCNTs/EG-water nanofluids. The PD and HTC were assessed using the correlations. It has been reported that the PD decreases as the shear rate increases, while it increases as the concentration and temperature increase. They determined that F-MWCNTs/EG-water nanofluids are an appropriate option for operating conditions with increased shear rates. Contreras et al. [42] examined flow and thermal efficiency of nanofluids made of graphene and silver dissolved in water for use in radiators of vehicles. They reported a 4.1% increase in pumping power at elevated temperatures and mass flow rates. They determined that the HT was enhanced by 4.4% with silver nanofluid, but the thermo-hydraulic efficacy was degraded with graphene nanofluid. A research was carried out by Abbas et al. [43] on use of  $\text{Fe}_2\text{O}_3$ - $\text{TiO}_2$ /water hybrid nanofluids into heat exchangers for aluminium tube vehicles. An experimental study was conducted with a flow rate of 11-15 LPM, an inlet temperature of 48 to 56°C, and operating conditions of 0.005, 0.007, and 0.009 vol%. The HT was reduced by 8% at the inlet temperature, and the performance was significantly reduced at higher concentrations owing to the unstable mixture. Contreras et al. [44] conducted an experimental study on radiators that operate at high temperatures, utilising the MWCNT nanofluid to adjust the concentration and inlet temperature. They practically assessed HT rate and HTC. The volume fraction increased heat transfer efficacy, but the inlet temperature decreased it.

This research aims to compare HTC between Plain Tube and twisted tube radiator the best nanofluid for automobile cooling systems and understand how operational circumstances like mass flow rates affect their performance. Despite significant advances in nanofluid research to increase vehicle radiator heat transfer, several questions remain.

Previous research has focused on the effects of specific nanofluids on heat transfer coefficients, without comparing different categories. In addition, the effects of mass flow rates on these nanofluids in car radiators are not well studied. Most study has concentrated on steady-state settings, ignoring dynamic mass flow rate variations in automobile operations. Comparing the heat transfer coefficients of  $\text{Al}_2\text{O}_3$ -water and CuO-water nanofluids at different mass flow rates will help build more efficient and dependable automobile cooling systems. This study addresses these gaps by comparing  $\text{Al}_2\text{O}_3$ -water and CuO-water nanofluids under different mass flow rates to better understand their heat transfer effects in vehicle radiators.

## 2. Experimental Setup and Experimentation:

Fig. 1 shows a systematic line diagram of an experimental setup, while Fig. 2 shows the real setup. This setup has been used to measure heat transfer coefficient of car radiator. This experimental setup includes a reservoir SS tank with insulator, electrical heater, a centrifugal pump, a flow meter, tubes, valves, a fan, a power supply; 8 thermocouples for temperature measurement, and two radiators, one conventional radiator with plain tube and another fitted with twisted tube. The Twisted tube radiator consists 12 vertical twisted tubes with oval cross section with inner diameter of 8 mm. An electrical heater of 1500W inside reservoir SS tank with insulator put to represent the engine and to heat the fluid. A flow meter of capacity 0 - 300 LPH and two valves used to measure and control the flow rate. The fluid flows through plastic tubes (8 mm.) By a centrifugal pump from the tank to the radiator at the flow rate range 0.5–3 LPM. The capacity of centrifugal pump is 0.5 HP. The total volume of the circulating fluid is constant in all the experimental steps. Two thermocouples have been fixed on the flow line for determining inlet and outlet fluid temperatures. Two thermocouples have been fixed to the radiator surface to measure wall temperature. The speed of a fan was kept constant throughout the experiments.

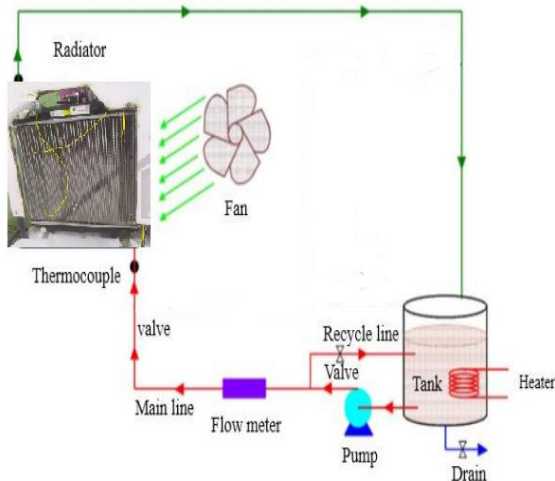


Fig. 1. Line diagram of experimental setup



Figure 2. Actual Experimental Setup

### 3. Results and discussion:

The research was conducted to improve the efficacy of the radiator, as previously mentioned. The radiator's convective HTC is the most effective parameter. The plain tube and twisted tube radiator's convective heat transmission coefficient was examined in this section. The investigation was conducted on two distinct nanofluids:  $Al_2O_3$  and  $CuO$ . The impact of mass flow rate upon a HTC as a function of the inlet fluid temperature was investigated in this section.

#### 3.1 Effect of mass flow rate on heat transfer Coefficient for Plain Tube Radiator.

##### 3.1.1 For Aluminum oxide + Water based Nano-fluid

The radiator of the car underwent testing using plain tubes, with experiments conducted using aluminum oxide and water-based nanofluid. Various mass flow rates of the nanofluid were tested, ranging from 0.5 liters per minute (lpm) to 3 lpm. The impact of mass flow rate upon convective HTC was analyzed for nanofluid concentrations of 0.3%, 0.5%, and 1% aluminum oxide, as depicted in Figures 3, 4, and 5, respectively. The inlet fluid temperature was varied from  $60^\circ C$  to  $120^\circ C$ .

Figure 3 illustrates the influence of mass flow rate and varying inlet fluid temperature upon a convective HTC for 0.3% nanofluid. At an inlet temperature of  $60^\circ C$  and a flow rate of 0.5 lpm, the minimum convective heat transfer observed was  $229.92 W/m^2K$ . However, with increment into mass flow rate at a same inlet temperature, a HTC also increases, reaching a maximum of  $2299.85 W/m^2K$ . It was noted that, at the constant inlet fluid temperature, an increase in mass flow rate led to a corresponding increase in the convective HTC. The highest heat transfer coefficients were consistently observed at 3 lpm across all inlet temperatures. Additionally, Figure 3 indicates that the maximum heat transfer coefficient among all inlet temperatures was achieved at  $80^\circ C$ , reaching  $3861.26 W/m^2K$  for a flow rate of 3 lpm.

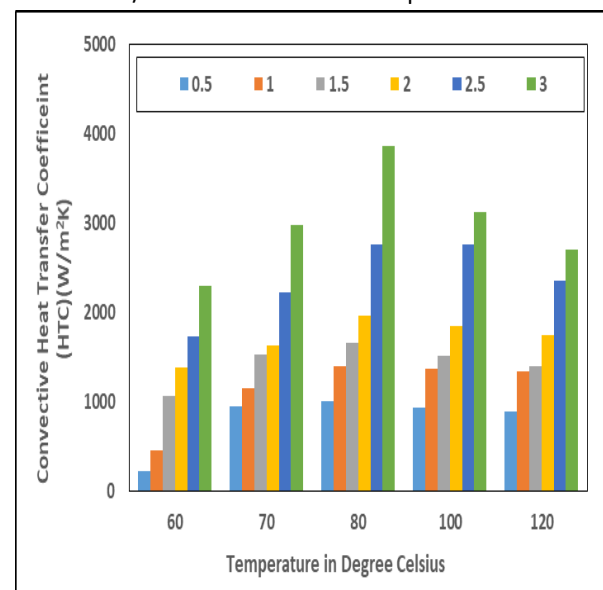
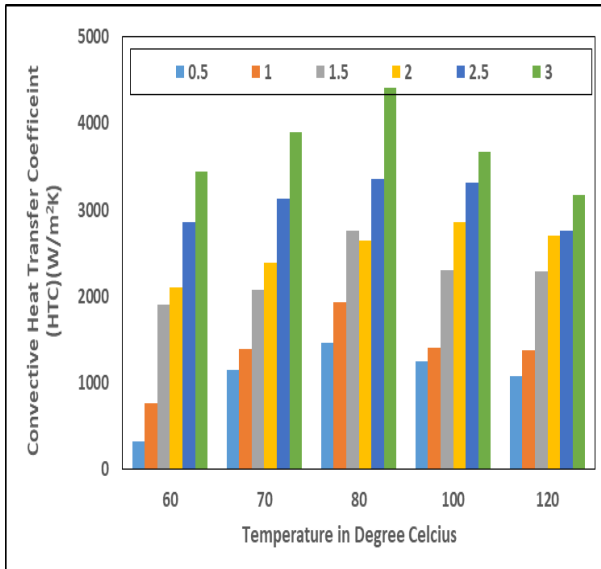


Figure 3. Effect of Mass Flow Rate with varying inlet fluid temperature at a 0.3%  $Al_2O_3$  Nanofluid



**Figure 4 Effect of Mass Flow Rate with varying inlet fluid temperature at a 0.5% Al<sub>2</sub>O<sub>3</sub> Nanofluid**

In Figure 4, the impact of mass flow rate upon a convective HTC for a 0.5% nanofluid is examined, considering varying inlet fluid temperatures. At an inlet temperature of 60°C and a mass flow rate of 0.5 lpm, the minimum convective HTC observed is 319.42 W/m<sup>2</sup>K. However, with an increase in mass flow rate at the same inlet temperature, a HTC also increases, reaching a maximum of 3446.11 W/m<sup>2</sup>K.

Consistent with the findings in Figure 3, it's observed that at a constant inlet fluid temperature, increasing the mass flow rate leads to a higher convective HTC. Across all inlet temperatures, the highest heat transfer coefficients are achieved at a mass flow rate of 3 lpm. Moreover, Figure 4 indicates that the maximum heat transfer coefficient among all inlet temperatures is attained at 80°C, reaching 4411.91 W/m<sup>2</sup>K for a flow rate of 3 lpm.

In Figure 5, the impact of mass flow rate upon a convective HTC for a 1% nanofluid is analyzed across varying inlet fluid temperatures. At an inlet temperature of 60°C and a mass flow rate of 0.5 lpm, the minimum convective HTC observed is 382.90 W/m<sup>2</sup>K. However, as the mass flow rate increases at the same inlet temperature, a HTC also increases, reaching a maximum of 4347.08 W/m<sup>2</sup>K.

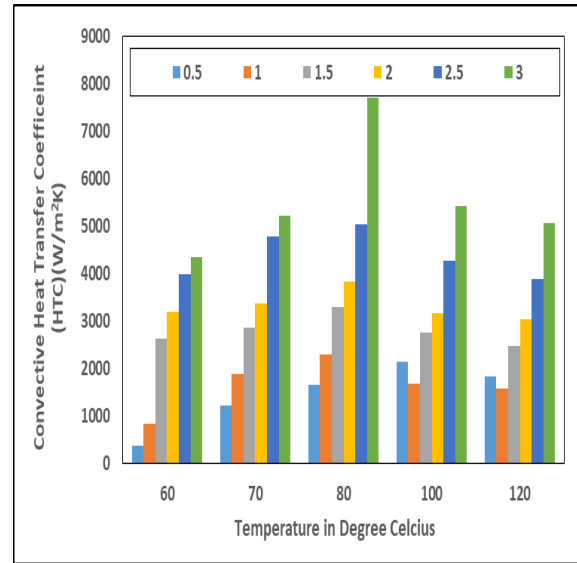


**Figure 5 Effect of Mass Flow Rate with varying inlet fluid temperature at a 1% Al<sub>2</sub>O<sub>3</sub> Nanofluid**

Consistent with the trends observed in Figures 3 and 4, it's noted that at a constant inlet fluid temperature, increment in mass flow rate leads to a higher convective HTC. Across all inlet temperatures, the maximum heat transfer coefficients are attained at a mass flow rate of 3 lpm. Additionally, Figure 5 highlights that among all inlet temperatures, the highest heat transfer coefficient is achieved at 80°C, reaching 7716.52 W/m<sup>2</sup>K for a flow rate of 3 lpm.

### 3.1.2 For Copper oxide + Water based Nano-fluid

The radiator of the car underwent testing using plain tubes, with experiments conducted using copper oxide and water-based nanofluid. Various mass flow rates of the nanofluid were tested, ranging from 0.5 liters per minute (lpm) to 3 lpm. The impact of mass flow rate upon convective HTC was analyzed for nanofluid concentrations of 0.3%, 0.5%, and 1% copper oxide, as depicted in Figures 6, 7, and 8, respectively. The inlet fluid temperature was varied from 60°C to 120°C.

In Figure 6, the impact of mass flow rate and varying inlet fluid temperature upon a convective HTC for a 0.3% nanofluid is analyzed.

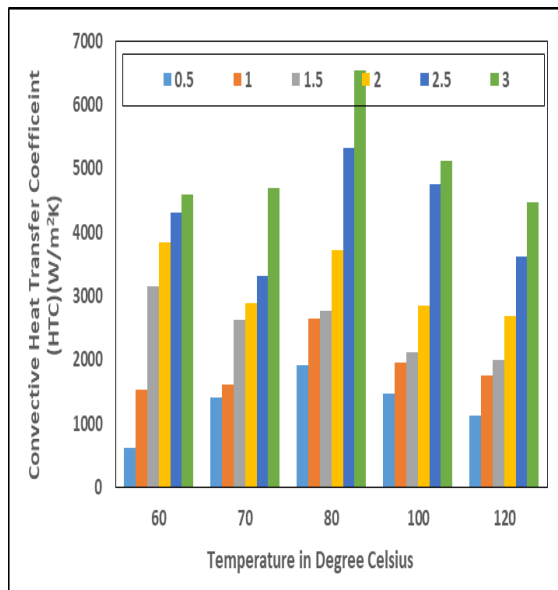


**Figure 6. Effect of Mass Flow Rate with varying inlet fluid temperature at a 0.3% CuONanofluid**

At an inlet temperature of 60°C and a mass flow rate of 0.5 lpm, the minimum convective HTC observed is 622.70 W/m<sup>2</sup>K. However, with an increase in mass flow rate at the same inlet temperature, a HTC also increases, reaching a maximum of 4599.70 W/m<sup>2</sup>K.

Consistent with the findings in previous figures, it's observed that at a constant inlet fluid temperature, increment in mass flow rate leads to a higher convective HTC. The maximum heat transfer coefficients are consistently achieved at a mass flow rate of 3 lpm for all tested inlet temperatures. Additionally, Figure 6 highlights that among all inlet temperatures, the maximum heat transfer coefficient is attained at 80°C, reaching 6543.35 W/m<sup>2</sup>K for a flow rate of 3 lpm.

In figure 7 it has observed that, the effect of mass flow rate with varying inlet fluid temperature upon convective HTC for 0.5% nanofluid. The minimum convective heat transfer observed at an inlet temperature of 60°C and at 0.5 lpm is 830.51 W/m<sup>2</sup>K. But at a similar intake temperature, HTC grows with mass flow rate and maximum HTC observed is 6322.81 W/m<sup>2</sup>K. It has been observed that, at a constant inlet fluid temperature, as mass flow rate increases a convective HTC increases. The maximum HTC obtain for all inlet temperature are for 3 lpm. The figure 7, also shows that, among all inlet temperature the maximum HTC obtain at 80°C i.e. 7065.93 W/m<sup>2</sup>K for 3 lpm.

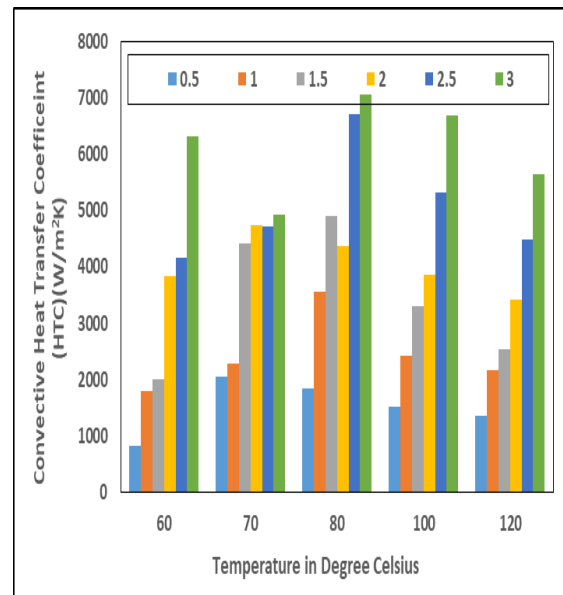


**Figure 7 Effect of Mass Flow Rate with varying inlet fluid temperature at a 0.5% CuONanofluid**

In Figure 8 it has observed that, the effect of mass flow rate with varying inlet fluid temperature upon convective HTC for 0.5% nanofluid. The minimum convective heat transfer observed at an inlet temperature of 60°C and at 0.5 lpm is 1531.67 W/m<sup>2</sup>K. But at a similar intake temperature, HTC grows with mass flow rate and maximum HTC observed is 7232.41 W/m<sup>2</sup>K. It has been observed that, at a constant inlet fluid temperature, as mass flow rate increases the convective HTC increases. The maximum HTC obtain for all inlet temperature are for 3 lpm. The figure 8, also shows that, among all inlet temperature the maximum HTC obtain at 80°C i.e. 10181.09 W/m<sup>2</sup>K for 3 lpm.

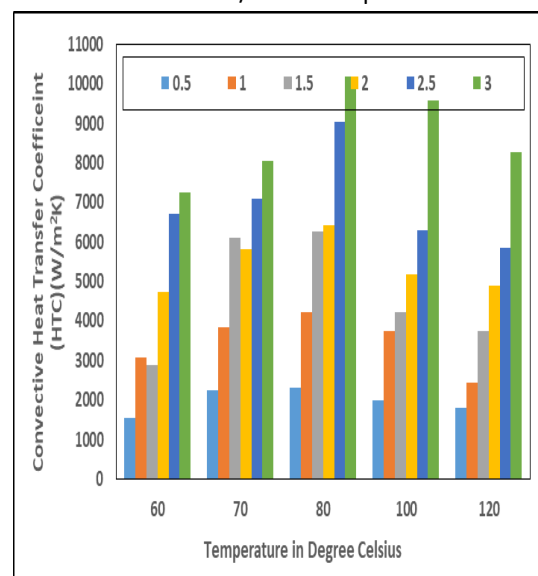


**Figure 8. Effect of Mass Flow Rate with varying inlet fluid temperature at a 1% CuONanofluid**

### 3.2 Effect of mass flow rate on heat transfer Coefficient for Twisted Tube Radiator

The research was conducted to improve the efficacy of the radiator, as previously mentioned. The radiator's convective heat transmission coefficient is the most effective parameter. The convective heat transmission coefficient for the twisted tube radiator was examined in this section. The investigation was conducted on two distinct nanofluids:  $\text{Al}_2\text{O}_3$  and  $\text{CuO}$ . A study was conducted in this section to investigate the impact of mass flow rate upon a HTC of a twisted tube radiator as the inlet fluid temperature varied.

#### 3.2.1. For Aluminum oxide + Water based Nano-fluid

The radiator of car was tested with twisted tubes. The testing was carried out for the Aluminum oxide and water based nanofluid. The different mass flow rates of nanofluid were consider for the testing those were 0.5 lpm, 1 lpm, 1.5 lpm, 2 lpm, 2.5 lpm and 3 lpm. The Effect of mass flow rate upon a convective HTC for twisted tube radiator were given in below Figure 9, 10 and 11 for 0.3%, 0.5% and 1% aluminum oxide nanofluid respectively. The inlet temperature of fluid was also varying from  $60^\circ\text{C}$  to  $120^\circ\text{C}$ .

In figure 9 it has observed that, the effect of mass flow rate with varying inlet fluid temperature upon convective HTC for 0.5% nanofluid.

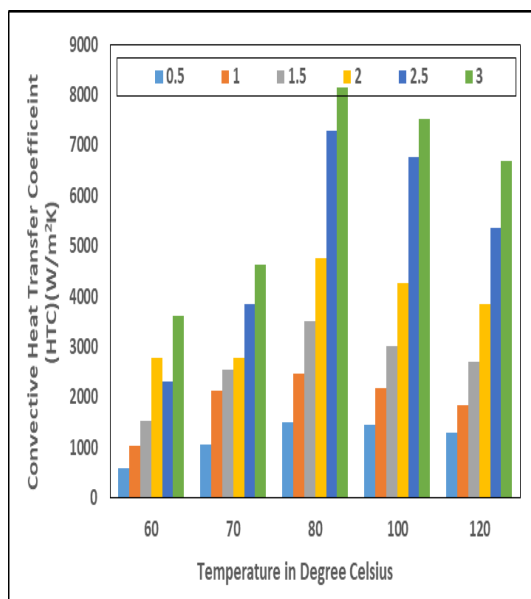


Figure 9. Effect of Mass Flow Rate with varying inlet fluid temperature at a 0.3%  $\text{Al}_2\text{O}_3$  Nanofluid

The minimum convective heat transfer observed at an inlet temperature of  $60^\circ\text{C}$  and at 0.5 lpm is

$579.46 \text{ W/m}^2\text{K}$ . But at a similar intake temperature, HTC grows with mass flow rate and maximum HTC observed is  $3617 \text{ W/m}^2\text{K}$ . It has been observed that, at a constant inlet fluid temperature, as mass flow rate increases a convective HTC increases. The maximum HTC obtain for all inlet temperature are for 3 lpm. The figure 9, also shows that, among all inlet temperature the maximum HTC obtain at  $80^\circ\text{C}$  i.e.  $8151.55 \text{ W/m}^2\text{K}$  for 3 lpm.

In figure 10 it has observed that, the effect of mass flow rate with varying inlet fluid temperature upon convective HTC for 0.5% nanofluid. The minimum convective heat transfer observed at an inlet temperature of  $60^\circ\text{C}$  and at 0.5 lpm is  $849.89 \text{ W/m}^2\text{K}$ . But at a similar intake temperature, HTC grows with mass flow rate and maximum HTC observed is  $4519.87 \text{ W/m}^2\text{K}$ . It has been observed that, at a constant inlet fluid temperature, as mass flow rate increases a convective HTC increases. The maximum HTC obtain for all inlet temperature are for 3 lpm. The figure 10, also shows that, among all inlet temperature the maximum HTC obtain at  $80^\circ\text{C}$  i.e.  $10478.29 \text{ W/m}^2\text{K}$  for 3 lpm.

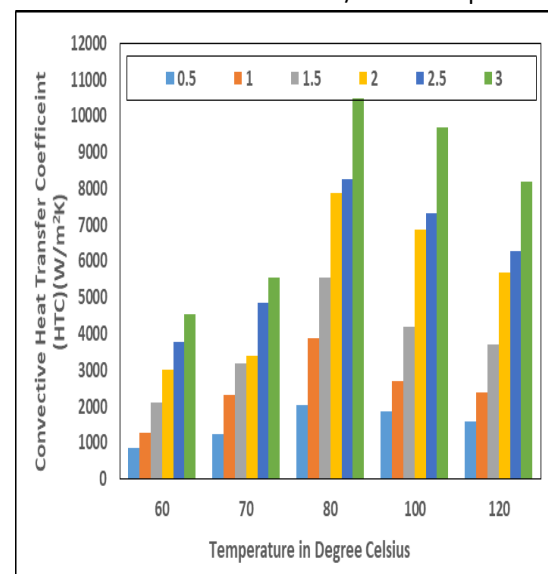
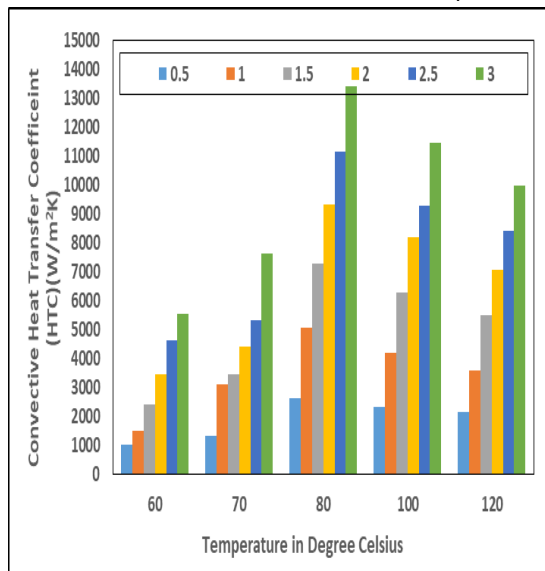


Figure 10 Effect of Mass Flow Rate with varying inlet fluid temperature at a 0.5%  $\text{Al}_2\text{O}_3$  Nanofluid

In figure 11 it has observed that, the effect of mass flow rate with varying inlet fluid temperature upon convective HTC for 0.5% nanofluid. The minimum convective heat transfer observed at an inlet temperature of  $60^\circ\text{C}$  and at 0.5 lpm is  $1003.65 \text{ W/m}^2\text{K}$ . But at a similar intake temperature, HTC grows with mass flow rate and maximum HTC observed is  $5558.69 \text{ W/m}^2\text{K}$ . It has been observed



that, at a constant inlet fluid temperature, as mass flow rate increases a convective HTC increases. The maximum HTC obtain for all inlet temperature are for 3 lpm. The figure 11, also shows that, among all inlet temperature the maximum HTC obtain at 80°C i.e. 13381.43 W/m<sup>2</sup>K for 3 lpm.



**Figure 11 Effect of Mass Flow Rate with varying inlet fluid temperature at a 1% Al<sub>2</sub>O<sub>3</sub> Nanofluid**

### 3.2.2. For Copper oxide + Water based Nano-fluid

The radiator of car was tested with twisted tubes. The testing was carried out for the Copper oxide and water based nanofluid. The different mass flow rates of nanofluid were consider for the testing those were 0.5 lpm, 1 lpm, 1.5 lpm, 2 lpm, 2.5 lpm and 3 lpm. The Effect of mass flow rate upon a convective HTC for twisted tube radiator were given in below Figure 12, 13 and 14 for 0.3%, 0.5% and 1% copper oxide nanofluid respectively. The inlet temperature of fluid was also varying from 60°C to 120°C.

In figure 12 it has observed that, the effect of mass flow rate with varying inlet fluid temperature upon convective HTC for 0.5% nanofluid. The minimum convective heat transfer observed at an inlet temperature of 60°C and at 0.5 lpm is 1016 W/m<sup>2</sup>K. But at a similar intake temperature, HTC grows with mass flow rate and maximum HTC observed is 6008.07 W/m<sup>2</sup>K. It has been observed that, at a constant inlet fluid temperature, as mass flow rate increases a convective HTC increases. The maximum HTC obtain for all inlet temperature are for 3 lpm. The figure 12, also shows that, among all inlet temperature the maximum HTC obtain at 80°C i.e. 8620.21 W/m<sup>2</sup>K for 3 lpm.

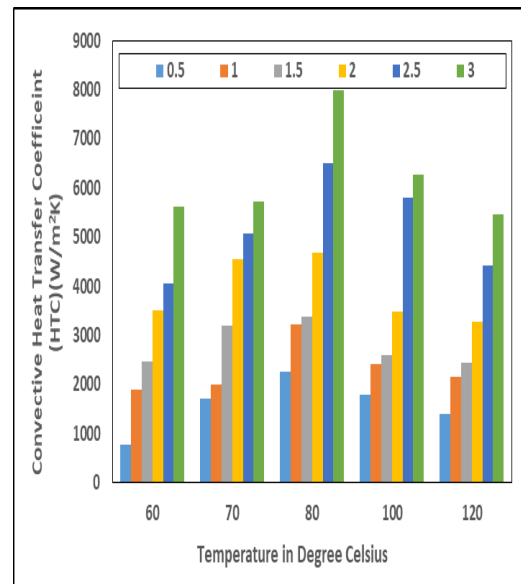


**Figure 12 Effect of Mass Flow Rate with varying inlet fluid temperature at a 0.3% CuONanofluid**

In figure 13 it has observed that, the effect of mass flow rate with varying inlet fluid temperature upon convective HTC for 0.5% nanofluid. The minimum convective heat transfer observed at an inlet temperature of 60°C and at 0.5 lpm is 1016 W/m<sup>2</sup>K. But at a similar intake temperature, HTC grows with mass flow rate and maximum HTC observed is 6008.07 W/m<sup>2</sup>K. It has been observed that, at a constant inlet fluid temperature, as mass flow rate increases a convective HTC increases. The maximum HTC obtain for all inlet temperature are for 3 lpm. The figure 13, also shows that, among all inlet temperature the maximum HTC obtain at 80°C i.e. 8620.21 W/m<sup>2</sup>K for 3 lpm.

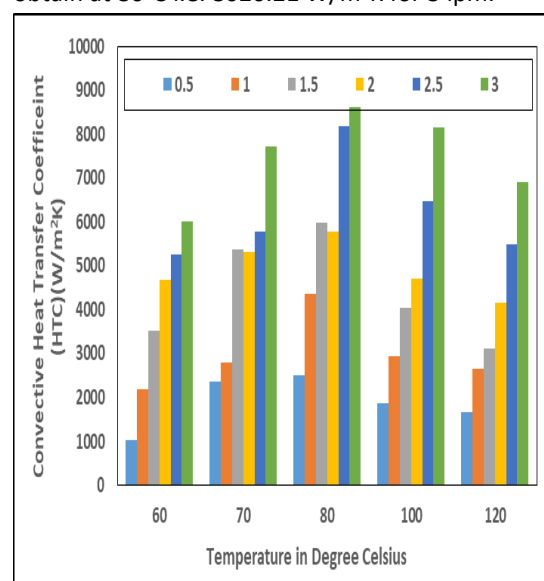


**Figure 13 Effect of Mass Flow Rate with varying inlet fluid temperature at a 0.5% CuONanofluid**



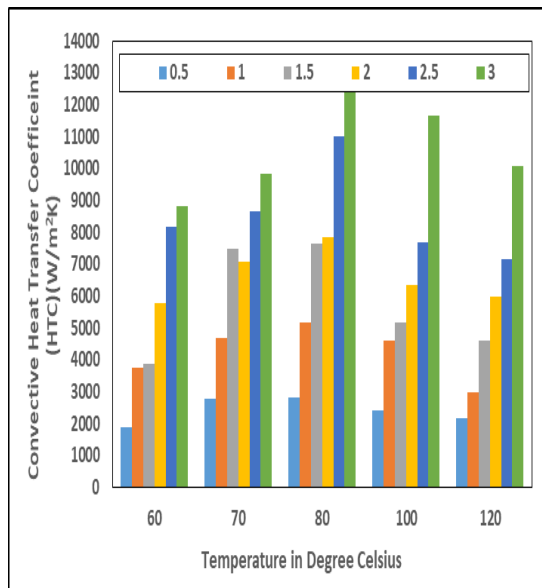


**Figure 14. Effect of Mass Flow Rate with varying inlet fluid temperature at a 1% CuONanofluid**

In figure 14 it has observed that, the effect of mass flow rate with varying inlet fluid temperature upon convective HTC for 0.5% nanofluid. The minimum convective heat transfer observed at an inlet temperature of 60°C and at 0.5 lpm is 1874.61 W/m<sup>2</sup>K. But at a similar intake temperature, HTC grows with mass flow rate and maximum HTC observed is 8827.98 W/m<sup>2</sup>K. It has been observed that, at a constant inlet fluid temperature, as mass flow rate increases a convective HTC increases. The maximum HTC obtain for all inlet temperature are for 3 lpm. The figure 14, also shows that, among all inlet temperature the maximum HTC obtain at 80°C i.e. 12429.33 W/m<sup>2</sup>K for 3 lpm.

### 3.3 Validation for heat transfer Coefficient for Twisted Tube Radiator

A multiple linear regression Mathematical model is generated to calculate the ratio of input to output by formulating the regression equation. By establishing a regression equation in this manner, a correlation is established between the significant conditions identified through ANOVA analysis, including the Change in Temp, % Concentration nanoparticle, Mass flow rate of nanofluid, Air velocity, Density, Dynamic viscosity, Sp. Heat, and Th. Conductivity.. Equation (1) and equation (2) provides the regression equation that was devised to determine a HTC for Al<sub>2</sub>O<sub>3</sub> and CuONanofluid respectively.

$$h = 121433.3 + 25770.61 \cdot C + 1952.241 \cdot m + 245.24 \cdot \text{Vair} + 73.7475 \cdot \rho - 7 \times 10^{-7} \cdot \mu + 4.644 \cdot C_p - 290505 \cdot k -$$

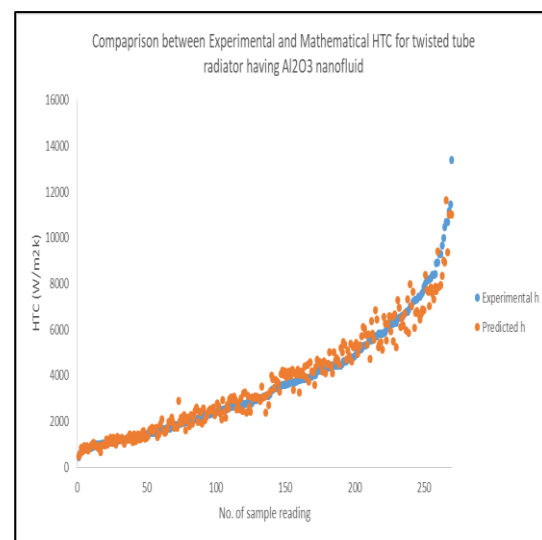
$$274.18 \cdot \Delta T$$

(1)

$$h = 85669.65 + 4600.45 \cdot C + 1980.65 \cdot m + 191.965 \cdot \text{Vair} - 43.9393 \cdot \rho + 3084627 \cdot \mu - 8.54842 \cdot C_p - 13728.7 \cdot k - 79.1875 \cdot \Delta T$$

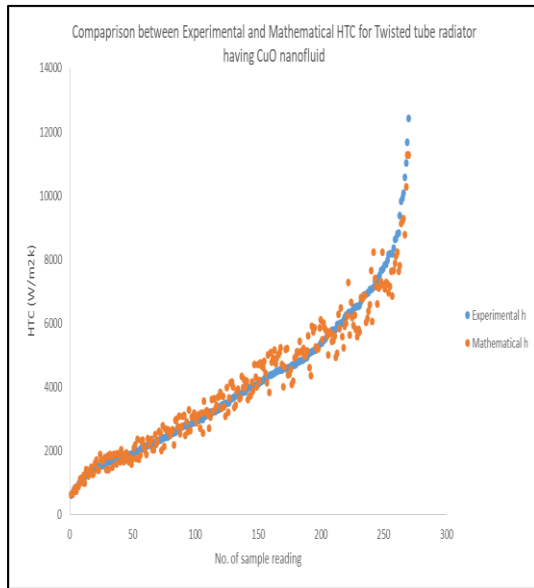
(2)

Figure 15 shows the comparison between Experimental and Mathematical heat transfer Coefficient for twisted tube radiator having Al<sub>2</sub>O<sub>3</sub> nanofluid. It is observed from figure 15 that Output produced by experimentation, and mathematical model is very close to each other. At few point they match with each other shows their closeness is quite high. Hence the values of actual experimentation conducted, and mathematical model formed is validated.



**Figure 15. Comparison between Experimental and Mathematical heat transfer Coefficient for twisted tube radiator having Al<sub>2</sub>O<sub>3</sub> nanofluid**

Figure 16 shows the comparison between Experimental and Mathematical heat transfer Coefficient for twisted tube radiator having CuONanofluid. It is observed from figure 16 that Output produced by experimentation, and mathematical model is very close to each other. At few point they match with each other shows their closeness is quite high. Hence the values of actual experimentation conducted, and mathematical model formed is validated.



**Figure 16. Comparison between Experimental and Mathematical heat transfer Coefficient for twisted tube radiator having CuO nanofluid**

#### Conclusions:

During the course of this study, a twisted tube radiator was designed to facilitate all aspects of cooling. During the course of the research, it was discovered that there was a chance of improving existing design of radiator. Because of this, the following conclusions can be drawn from the current research:

1. After studying the literature, it is found that twisted tube type heat exchangers reveals numerous advantages over traditional shell and tube heat exchangers with segmental baffles. These advantages include superior construction, thermal properties, performance, and application flexibility. Twisted tube heat exchangers offer higher economic performance, as evidenced by their cost-effectiveness per unit of heat load compared to traditional equipment.
2. Experimental Observation conducted revealed that car radiator with Twisted tube has more HTC than Car radiator with plane tube across all nanofluid concentrations (0.3%, 0.5%, and 1%), and the mass flow rates.
3. From literature survey it is also noted that, the potential of nanofluids as coolant in automobile radiators presents promising opportunities for enhanced heat transfer, compact design, improved fuel economy, and reduced vehicle weight.

4. Across all nanofluid concentrations (0.3%, 0.5%, and 1%), it is evident that increasing the mass flow rate leads to a corresponding increase in the convective HTC. This relationship holds true for varying inlet fluid temperatures ranging from 60°C to 120°C.

5. The highest convective HTCs are consistently observed at a mass flow rate of 3 liters per minute (lpm) for all nanofluid concentrations and across all tested inlet temperatures. This suggests that higher flow rates enhance heat transfer efficiency.

6. The maximum convective HTCs are found at 80°C for all nanofluid concentrations and flow rates in both plain and twisted tube car radiator. This represents heat transfer efficiency's best working condition.

7. Both CuO and Al<sub>2</sub>O<sub>3</sub> nanofluids improve heat transmission. CuO nanofluid outperforms Al<sub>2</sub>O<sub>3</sub> at greater air velocities, with an 8% higher heat transfer coefficient.

8. These findings affect radiator design and optimization in vehicle cooling systems. CuO nanofluid may improve heat transfer efficiency, enhancing cooling and system performance.

9. The study shows that nanofluids can improve heat transfer and offers implications for radiator design and thermal management systems. Future research could optimize nanofluid compositions, flow configurations, and operational parameters to improve heat transfer performance and efficiency.

#### References:

1. Kaleli, A.: Development of the predictive based control of an autonomous engine cooling system for variable engine operating conditions in SI engines: design, modeling and real-time application. *Control Eng. Pract.* 100, 104424 (2020).  
<https://doi.org/10.1016/j.conengprac.2020.104424>
2. Sadeghianjahromi, A., Wang, C.-C.: Heat transfer enhancement in fin-and-tube heat exchangers – A review on different mechanisms. *Renew. Sustain. Energy Rev.* 137, 110470 (2021).  
<https://doi.org/10.1016/j.rser.2020.110470>

3. Li, W., Dai, R., Zeng, M., Wang, Q.: Review of two types of surface modification on pool boiling enhancement: Passive and active. *Renew. Sustain. Energy Rev.* 130, 109926 (2020).  
<https://doi.org/10.1016/j.rser.2020.109926>
4. Soudagar, M.E.M., Ramesh, S., Khan, T.M.Y., Almakayel, N., Ramesh, R., Ghazali, N.N.N., Cuce, E., Shelare, S.: An overview of the existing and future state of the art advancement of hybrid energy systems based on PV-solar and wind. *Int. J. Low-Carbon Technol.* 19, 207–216 (2024). <https://doi.org/10.1093/ijlct/ctad123>
5. Shelare, S.D., Aglawe, K.R., Belkhode, P.N.: A review on twisted tape inserts for enhancing the heat transfer. *Mater. Today Proc.* 54, 560–565 (2022).  
<https://doi.org/10.1016/j.matpr.2021.09.012>
6. Huang, Y., Xiao, X., Kang, H., Lv, J., Zeng, R., Shen, J.: Thermal management of polymer electrolyte membrane fuel cells: A critical review of heat transfer mechanisms, cooling approaches, and advanced cooling techniques analysis. *Energy Convers. Manag.* 254, 115221 (2022).  
<https://doi.org/10.1016/j.enconman.2022.115221>
7. Gupta, A., Kumar, R., Maurya, A., Ahmadi, M.H., Ongar, B., Yegzekova, A., Sharma, J.P., Kanchan, S., Shelare, S.: A comparative study of the impact on combustion and emission characteristics of nanoparticle-based fuel additives in the internal combustion engine. *Energy Sci. Eng.* (2023).  
<https://doi.org/10.1002/ese3.1614>
8. Shelare, S.D., Belkhode, P.N., Nikam, K.C., Jathar, L.D., Shahapurkar, K., Soudagar, M.E.M., Veza, I., Khan, T.M.Y., Kalam, M.A., Nizami, A.-S., Rehan, M.: Biofuels for a sustainable future: Examining the role of nano-additives, economics, policy, internet of things, artificial intelligence and machine learning technology in biodiesel production. *Energy.* 282, 128874 (2023).  
<https://doi.org/10.1016/j.energy.2023.128874>
9. Kapicioğlu, A., Esen, H.: Experimental investigation on using Al<sub>2</sub>O<sub>3</sub>/ethylene glycol-water nano-fluid in different types of horizontal ground heat exchangers. *Appl. Therm. Eng.* 165, 114559 (2020).  
<https://doi.org/10.1016/j.applthermaleng.2019.114559>
10. Mousa, M.H., Yang, C.-M., Nawaz, K., Miljkovic, N.: Review of heat transfer enhancement techniques in two-phase flows for highly efficient and sustainable cooling. *Renew. Sustain. Energy Rev.* 155, 111896 (2022).  
<https://doi.org/10.1016/j.rser.2021.111896>
11. Lv, H., Ma, H., Mao, N., He, T.: Boiling heat transfer mechanism of environmental-friendly refrigerants: A review. *Int. J. Refrig.* 133, 214–225 (2022).  
<https://doi.org/10.1016/j.ijrefrig.2021.10.007>
12. Waghmare, S.N., Shelare, S.D., Bahl, S., Mungle, N., Kumar Bagha, A., Chandmal Sharma, R.: Structural design and its analysis of two station notching tool for industrial die. *Mater. Today Proc.* 68, 1335–1341 (2022).  
<https://doi.org/10.1016/j.matpr.2022.06.360>
13. Arora, N., Gupta, M.: An updated review on application of nanofluids in flat tubes radiators for improving cooling performance. *Renew. Sustain. Energy Rev.* 134, 110242 (2020).  
<https://doi.org/10.1016/j.rser.2020.110242>
14. Shelare, S.D., Aglawe, K.R., Matey, M.S., Shelke, K.S., Sakhale, C.N.: Preparation, applications, challenges and future prospects of nanofluid materials with a solar systems in the last decade. *Mater. Today Proc.* (2023).  
<https://doi.org/10.1016/j.matpr.2023.06.160>
15. Soudagar, M.E.M., Shelare, S., Marghade, D., Belkhode, P., Nur-E-Alam, M., Kiong, T.S., Ramesh, S., Rajabi, A., Venu, H., Yunus Khan, T.M., Mujtaba, M., Shahapurkar, K., Kalam, M., Fattah, I.M.R.: Optimizing IC engine efficiency: A comprehensive review on biodiesel, nanofluid, and the role of artificial intelligence and machine learning. *Energy Convers. Manag.* 307, 118337 (2024).  
<https://doi.org/10.1016/j.enconman.2024.118337>
16. Ponangi, B.R., Krishna, V., Seetharamu, K.N.: Performance of compact heat exchanger in the presence of novel hybrid graphene nanofluids. *Int. J. Therm. Sci.* 165, 106925 (2021).

- <https://doi.org/10.1016/j.ijthermalsci.2021.106925>
17. Ukueje, W.E., Abam, F.I., Obi, A.: A Perspective Review on Thermal Conductivity of Hybrid Nanofluids and Their Application in Automobile Radiator Cooling. *J. Nanotechnol.* 2022, 1–51 (2022). <https://doi.org/10.1155/2022/2187932>
  18. Gajbhiye, T.S., Nikam, K.C., Kaliappan, S., Patil, P.P., Dhal, P.K., Pandian, C.K.A.: Sustainable renewable energy sources and solar mounting systems for PV panels: A critical review. In: *AIP Conference Proceedings*. p. 020066 (2023)
  19. Charyulu, D.G., Singh, G., Sharma, J.K.: Performance evaluation of a radiator in a diesel engine—a case study. *Appl. Therm. Eng.* 19, 625–639 (1999). [https://doi.org/10.1016/S1359-4311\(98\)00064-7](https://doi.org/10.1016/S1359-4311(98)00064-7)
  20. Rahmatinejad, Z., Tohidinezhad, F., Rahmatinejad, F., Eslami, S., Pourmand, A., Abu-Hanna, A., Reihani, H.: Internal validation and comparison of the prognostic performance of models based on six emergency scoring systems to predict in-hospital mortality in the emergency department. *BMC Emerg. Med.* 21, 68 (2021). <https://doi.org/10.1186/s12873-021-00459-7>
  21. Ben Hamida, M.B., Hatami, M.: Investigation of heated fins geometries on the heat transfer of a channel filled by hybrid nanofluids under the electric field. *Case Stud. Therm. Eng.* 28, 101450 (2021). <https://doi.org/10.1016/j.csite.2021.101450>
  22. J.A.A., S.A., I.V.I., E.A.O., I.D., A.O.J.: Finite Element Analysis to Predict Temperature and Velocity Distribution in Radiator Tubes. *Int. J. Eng. Manag. Res.* 9, 102–116 (2019). <https://doi.org/10.31033/ijemr.9.4.16>
  23. Bilen, K., Cetin, M., Gul, H., Balta, T.: The investigation of groove geometry effect on heat transfer for internally grooved tubes. *Appl. Therm. Eng.* 29, 753–761 (2009). <https://doi.org/10.1016/j.applthermaleng.2008.04.008>
  24. Murugesan, P., Mayilsamy, K., Suresh, S.: Turbulent Heat Transfer and Pressure Drop in Tube Fitted with Square-cut Twisted Tape. *Chinese J. Chem. Eng.* 18, 609–617 (2010). [https://doi.org/10.1016/S1004-9541\(10\)60264-9](https://doi.org/10.1016/S1004-9541(10)60264-9)
  25. Gajbhiye, T.S., Waghmare, S.N., Sirsat, P.M., Borkar, P., Awatade, S.M.: Role of nanomaterials on solar desalination systems: A review. *Mater. Today Proc.* (2023). <https://doi.org/10.1016/j.matpr.2023.04.532>
  26. Eiamsa-ard, S., Promvong, P.: Thermal characteristics of turbulent rib-grooved channel flows. *Int. Commun. Heat Mass Transf.* 36, 705–711 (2009). <https://doi.org/10.1016/j.icheatmasstransfer.2009.03.025>
  27. Gajbhiye, T., Shelare, S., Aglawe, K.: Current and Future Challenges of Nanomaterials in Solar Energy Desalination Systems in Last Decade. *Transdiscipl. J. Eng. Sci.* 13, 187–201 (2022). <https://doi.org/10.22545/2022/00217>
  28. Laohalertdecha, S., Wongwises, S.: The effects of corrugation pitch on the condensation heat transfer coefficient and pressure drop of R-134a inside horizontal corrugated tube. *Int. J. Heat Mass Transf.* 53, 2924–2931 (2010). <https://doi.org/10.1016/j.ijheatmasstransfer.2010.01.037>
  29. Gajbhiye, T.S., Waghmare, S., Dhande, M., Gondane, R., Giripunje, M., Shelare, S., Belkhole, P.: Polymer composite additive manufacturing: Applications, challenges and opportunities. *Mater. Today Proc.* (2024). <https://doi.org/10.1016/j.matpr.2024.06.013>
  30. Ji, W.-T., Jacobi, A.M., He, Y.-L., Tao, W.-Q.: Summary and evaluation on single-phase heat transfer enhancement techniques of liquid laminar and turbulent pipe flow. *Int. J. Heat Mass Transf.* 88, 735–754 (2015). <https://doi.org/10.1016/j.ijheatmasstransfer.2015.04.008>
  31. Mohammed, H.A., Al-Shamani, A.N., Sheriff, J.M.: Thermal and hydraulic characteristics of turbulent nanofluids flow in a rib-groove channel. *Int. Commun. Heat Mass Transf.* 39, 1584–1594 (2012). <https://doi.org/10.1016/j.icheatmasstransfer.2012.10.020>

32. Shelare, S.D., Aglawe, K.R., Giri, S.S., Waghmare, S.N.: Additive Manufacturing of Polymer Composites : Applications , Challenges and opportunities. *Indian J. Eng. Mater. Sci.* 30, 872–881 (2023). <https://doi.org/10.56042/ijems.v30i6.4490>
33. Belkhode, P.N., Afsar, A., Shelare, S., Borkar, K., Washimkar, P.: Investigation of two stroke engine to improve the brake power and thermal efficiency through the mathematical modeling approach. *AIP Conf. Proc.* 2800, 20152 (2023). <https://doi.org/10.1063/5.0163007>
34. Ajeel, R.K., W. Salim, W.-I., Hasnan, K.: Thermal and hydraulic characteristics of turbulent nanofluids flow in trapezoidal-corrugated channel: Symmetry and zigzag shaped. *Case Stud. Therm. Eng.* 12, 620–635 (2018). <https://doi.org/10.1016/j.csite.2018.08.002>
35. Tupkar, R., Kumar, D., Sakhale, C.: Material selection and parametric evaluation for medium duty belt conveyor: A review on current status and future directions. *Mater. Today Proc.* (2024). <https://doi.org/10.1016/j.matpr.2024.04.021>
36. Kocheril, R., Elias, J.: Comparison of heat transfer rate with aluminium based nano fluid and magnetised ferro fluid in internal combustion engine heat exchanger. *J. Adv. Res. Fluid Mech. Therm. Sci.* 67, 170–177 (2020)
37. Belkhode, P., Giripunje, M., Dhande, M., Gajbhiye, T., Waghmare, S., Tupkar, R., Gondane, R.: Nanomaterials applications in solar energy: Exploring future prospects and challenges. *Mater. Today Proc.* (2024). <https://doi.org/10.1016/j.matpr.2024.04.035>
38. Salamon, V., Senthil kumar, D., Thirumalini, S.: Experimental Investigation of Heat Transfer Characteristics of Automobile Radiator using TiO<sub>2</sub> -Nanofluid Coolant. *IOP Conf. Ser. Mater. Sci. Eng.* 225, 012101 (2017). <https://doi.org/10.1088/1757-899X/225/1/012101>
39. Goudarzi, K., Jamali, H.: Heat transfer enhancement of Al<sub>2</sub>O<sub>3</sub>-EG nanofluid in a car radiator with wire coil inserts. *Appl. Therm. Eng.* 118, 510–517 (2017). <https://doi.org/10.1016/j.applthermaleng.2017.03.016>
40. Said, Z., El Haj Assad, M., Hachicha, A.A., Bellos, E., Abdelkareem, M.A., Alazaizeh, D.Z., Yousef, B.A.A.: Enhancing the performance of automotive radiators using nanofluids. *Renew. Sustain. Energy Rev.* 112, 183–194 (2019). <https://doi.org/10.1016/j.rser.2019.05.052>
41. Shahsavani, E., Afrand, M., Kalbasi, R.: Using experimental data to estimate the heat transfer and pressure drop of non-Newtonian nanofluid flow through a circular tube: Applicable for use in heat exchangers. *Appl. Therm. Eng.* 129, 1573–1581 (2018). <https://doi.org/10.1016/j.applthermaleng.2017.10.140>
42. Cárdenas Contreras, E.M., Oliveira, G.A., Bandarra Filho, E.P.: Experimental analysis of the thermohydraulic performance of graphene and silver nanofluids in automotive cooling systems. *Int. J. Heat Mass Transf.* 132, 375–387 (2019). <https://doi.org/10.1016/j.ijheatmasstransfer.2018.12.014>
43. Abbas, F., Ali, H.M., Shaban, M., Janjua, M.M., Shah, T.R., Doranehgard, M.H., Ahmadiouydarab, M., Farukh, F.: Towards convective heat transfer optimization in aluminum tube automotive radiators: Potential assessment of novel Fe<sub>2</sub>O<sub>3</sub>-TiO<sub>2</sub>/water hybrid nanofluid. *J. Taiwan Inst. Chem. Eng.* 124, 424–436 (2021). <https://doi.org/10.1016/j.jtice.2021.02.002>
44. Cardenas Contreras, E.M., Bandarra Filho, E.P.: Heat transfer performance of an automotive radiator with MWCNT nanofluid cooling in a high operating temperature range. *Appl. Therm. Eng.* 207, 118149 (2022). <https://doi.org/10.1016/j.applthermaleng.2022.118149>